

# Enhanced Resolution Fiber Optic Strain Sensor Based on Mach-Zehnder Interferometer and Displacement Sensing Principles

Navid M.S. Jahed\*, Tofiq Nurmohammadi, Saeed Ounie\*, Rasoul Sadighi Bonabi\*

\* Sharif University of Technology, Tehran, Iran

[navid.jahed@ee.sharif.ir](mailto:navid.jahed@ee.sharif.ir), [tofiqurmohammadi@gmail.com](mailto:tofiqurmohammadi@gmail.com), [ounie\\_saeed@ee.sharif.ir](mailto:ounie_saeed@ee.sharif.ir), [sadighi@sharif.ir](mailto:sadighi@sharif.ir)

## Abstract

*In this study, a novel scheme for fiber optic strain sensor has been introduced. This scheme is indeed a Mach-Zehnder interferometer followed by a displacement sensor. The strain is applied to an optical fiber which is the main branch of the Mach-Zehnder interferometer and causes an alteration in the interferometer's output intensity. The output beam is then spread on a mirror located in front of the fiber head. The head of the fiber and the mirror form a displacement sensor configuration. The portion of the reflected beam, gathered by the fiber, is a function of the distance between the fiber head and the mirror. So, applying strain causes a new change in the gathered intensity due to the elongation of the fiber. The combination of the several effects in altering the detected power by variation in the applied strain makes the proposed sensor more sensitive.*

## 1. Introduction

The development of fiber optic sensors based on white light interferometry has been attractive in recent years [1,2]. There have been discussions in several recent articles on the use of such techniques for distributed strain or temperature sensing in advanced composite or other structural materials [3–6].

Due to its immunity to electromagnetic interference (EMI), especially in noisy environments, fiber optic strain sensors have been attractive in the past few years. Common electrical strain gauges have a low electrical output level and desensitizing these gauges to EMI is a difficult task. Several different types of fiber optic strain sensors have been reported by several groups of researchers [7].

Although interferometric sensors provide high resolution, but these sensors suffer the phase ambiguity of interferometric phase reading and the cross-

sensitivity effect in simultaneous measurement of measurands. Low coherence interferometric methods have been used to overcome those effects. Unfortunately the techniques require complicated output signal processing in comparison to high coherence sensors [8, 9]. Accuracy of measurement in such systems depends upon the extraction of phase from the interferogram.

In our proposed strain sensor configuration, the applied strain causes the variation of light intensity in two ways. First, the strained fiber of the main branch of a Mach-Zehnder interferometer exhibits length variation, so the superposed light intensity at the output of the Mach-Zehnder interferometer is proportional to the strain. This variation of intensity due to the phase shift results from the elongation of the fiber. Second, the length variation in fiber reduces the distance between the head of the fiber and the fixed mirror which in turn leads to intensity variation of the light. We also consider the changes of the refraction index due to the strain caused by length variation.

## 2. Principle of Fiber Optic Strain Sensor

The structure of the fiber optic strain sensor is depicted in Figure 1. The main part of the sensor is based on Mach-Zehnder interferometer. The Mach-Zehnder interferometer, invented over one hundred years ago, is still used for many optical measurements. A Mach-Zehnder interferometer is formed from two couplers connected by two arms of unequal optical lengths. The light is split in two arms of the input coupler of the interferometer and they are later recombined at the output coupler.

In this proposed sensor structure, the length difference of the two arms is due to the applied strain on the main arm. The unequal length of the arms causes the phase difference between the split beam which is a function of wavelength and arm length difference. So the intensity of the output beam contains

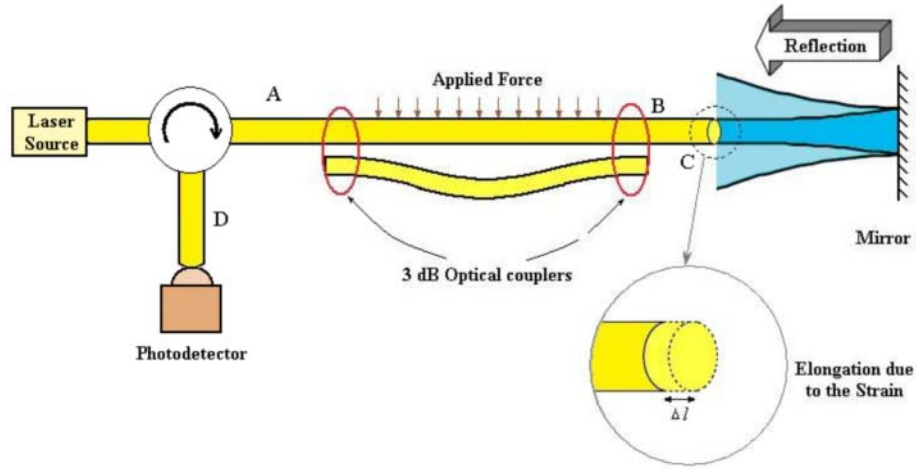


Figure 1. Configuration of the proposed fiber optic strain sensor

To improve the resolution we have to increase the sensitivity of the intensity to the applied strain. Therefore, we use a Mach-Zehnder interferometer followed by a displacement sensing system. In contrast to the ordinary displacement sensors, in our proposed system, the reflecting mirror is fixed so that we can measure the displacement of the head of fiber as illustrated in the zoomed part of Figure 1. It's overt that the gathered beam intensity is a function of the fiber elongation.

The reflected beam passes through the Mach-Zehnder and has been affected again by the strain. The Mach-Zehnder affects the reflected light similar to the foregoing light by changing the phase of the light field. In addition, the applied strain alters the refractive index of the optical fiber which leads to a change in the optical path.

So the improvement of the precision is due to the four strain effects: 1) The input light is affected by the elongation of the main arm of the Mach-Zehnder, 2) The elongation of the fiber modifies the intensity of the reflected beam, 3) Mach-Zehnder does have an effect on the reflected light as well as on the input light, and finally 4) The optical path varies because of the changes in refractive index.

### 3. Mathematical Equations

As explained in section 2, applied strain affects the sensor in four steps. By obtaining the mathematical equation for each step and multiplying them together, we can get the overall strain effect on the light intensity. Assuming that the Mach-Zehnder interferometer effect on reflected beam is similar to the input light; we only consider the main three steps.

#### 3.1. Mach-Zehnder Effect

The intensity of recombined light at the output of the coupler is obtained as follows:

$$I = I_1 + I_2 + 2\sqrt{I_1 I_2} \cos \varphi \quad (1)$$

Where  $I_1$  and  $I_2$  are the light intensity in the main and secondary arms respectively, and  $\varphi$  is the phase difference of the split beams which is defined as follows:

$$\varphi = \frac{n\Delta l}{\lambda} 2\pi \quad (2)$$

When  $I_1$  and  $I_2$  are equal (i.e.  $I_1 = I_2 = I_0$ ), (1) reduces to the following form:

$$I = 2I_0 \left( 1 + \cos \left( \frac{n\Delta l}{\lambda} 2\pi \right) \right) \quad (3)$$

So the light power in the cross section of the fiber at the point B can be written as:

$$P_B = \frac{1}{2} P_A \left( 1 + \cos \left( \frac{n\Delta l}{\lambda} 2\pi \right) \right) \quad (4)$$

Similarly, one can see that the light power at the point D is:

$$P_D = \frac{1}{2} P_C \left( 1 + \cos \left( \frac{n\Delta l}{\lambda} 2\pi \right) \right) \quad (5)$$

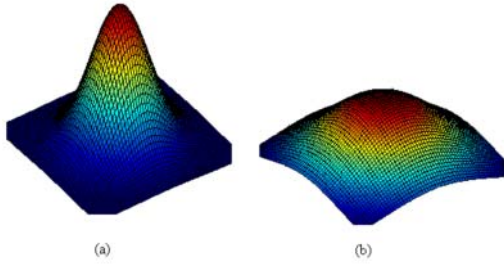


Figure 2. (a) Light intensity at the output of the fiber. (b) Intensity of the reflected light.

### 3.2. Displacement Sensor Block

The intensity distribution of the input beam and the reflected one is shown in Figure 2. It can be seen that the intensity in the input is focused in the center, but the intensity in the reflected one is scattered and is a function of the distance between the object and the fiber, so as the displacement of the fiber. Considering Gaussian distribution for the input beam the intensity as a function of  $z$  (the distance) is obtained as follows [10, 11]

$$I(r, z) = A \frac{a^2}{w^2(z)} \exp\left[-\frac{2r^2}{w^2(z)}\right]. \quad (6)$$

$A$ ,  $w(z)$  and  $z_0$  are defined as

$$w(z) \triangleq a \sqrt{1 + \frac{z^2}{z_0^2}} \quad (7)$$

$$z_0 \triangleq \frac{ka^2}{2} \quad (8)$$

$$A = \frac{\sqrt{2}}{\pi^{3/2}} \frac{1}{a} \quad (9)$$

where  $a$  is the fiber diameter and  $A$  is a normalization constant. So the intensity of the fraction of reflected beam gathered by the fiber is obtained as follows

$$P_r(\Delta l) = 2\pi \int_0^a I(r, 2(d - \Delta l)) \cdot dr \quad (10)$$

where  $d$  is the distance between the fiber head and the mirror.

By substituting (4) in (7) we obtain

$$P_r(\Delta l) = 2\pi A \frac{a^2}{w^2(z)} \int_0^a \exp\left[-\frac{2r^2}{w^2(z)}\right] \cdot dr \quad (11)$$

Where

$$z = 2(d - \Delta l). \quad (12)$$

By defining the error function as:

$$\text{erf}(x) = \frac{2}{\sqrt{\pi}} \int_0^x e^{-t^2} dt \quad (13)$$

(8) can be expressed in the following form:

$$P_r(\Delta l) = \pi \sqrt{\frac{\pi}{2}} A \frac{a^2}{w(z)} \cdot \text{erf}\left(\frac{\sqrt{2}}{w(z)} a\right). \quad (14)$$

Therefore, the light power at the point C is

$$P_C = P_B \frac{a}{w(z)} \cdot \text{erf}\left(\frac{\sqrt{2}}{w(z)} a\right). \quad (15)$$

### 3.3 Refractive Index

The applied strain also causes variations in refractive index. The overall equivalent refractive index of the core has simple algebraic forms as:

$$n_{eq} = n + \Delta n \quad (16)$$

where  $\Delta n$  is the variation in the refractive index [10]

$$\Delta n = -\frac{1}{2} n^3 [(p_{12} + p_{11})\varepsilon_l - p_{11}\varepsilon_a] \quad (17)$$

in which  $\varepsilon_l$  and  $\varepsilon_a$  are respectively lateral and axial strains, and  $P_{11}$  and  $P_{12}$  are Pockels constants. The Poisson effect,

$$\varepsilon_l = \mu \varepsilon_a \quad (18)$$

Eq. (17) can be written in the following form

$$\Delta n = -\frac{1}{2} n^3 [(1 - \mu)p_{12} - \mu p_{11}]\varepsilon \quad (19)$$

where  $\mu$  is the Poisson's ratio.

So (16) becomes as follows:

$$n_{equivalent} = n - \frac{1}{2} n^3 [(1 - \mu)p_{12} - \mu p_{11}]\varepsilon. \quad (20)$$

For silicon materials at wavelength = 1550 nm , the parameters are  $n = 1.46$  ,  $\mu = 0.25$  ,  $p_{11} \approx 0.12$

,  $p_{12} \approx 0.76$  [11].

### 3.4 Total Detected Power

Using the results of the three previous sections, we can deduce the variation of the detected power by the change in applied strain. Combining (4), (5), (15) and (20) we can obtain the following equation:

$$P_D = P_r(\Delta l) = \left[ \frac{P_0}{\text{erf}(\sqrt{2})} \frac{a}{w(z)} \cdot \text{erf}\left(\frac{\sqrt{2}}{w(z)} a\right) \right] \times \left[ \frac{1}{2} \left( 1 + \cos\left(\frac{n_{eq} \Delta l}{\lambda} 2\pi\right) \right) \right]^2 \quad (21)$$

where  $w(z)$  and  $n_{eq}$  have been defined in (7) and (16), respectively.

## 4. Numerical Results

In this section the numerical results and some discussions. The purpose of the results is to illustrate the precision of the proposed system. Here, we find the characteristics curve of the proposed fiber-optic strain sensor.

By setting  $a=10\mu\text{m}$ ,  $\lambda=1.55\mu\text{m}$  and  $l=10\text{ cm}$  in (21) we obtain the characteristics curve of the sensor as shown in Figure 3. In this figure, the characteristics curve of the displacement sensing part is illustrated by the dashed line which is obtained from Eq. (15). The solid line is the total received normalized power in which we have taken into account all of the effects mentioned above.

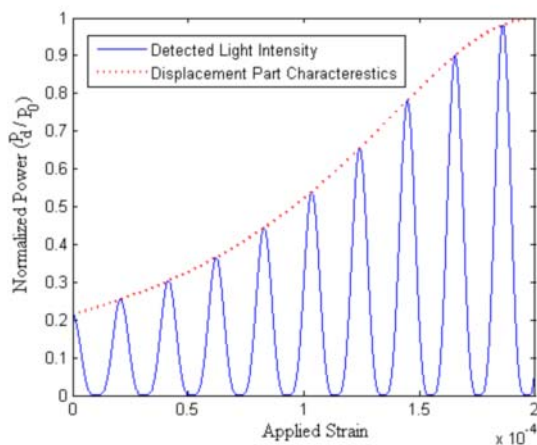


Figure 3. The characteristics curves of the displacement part (dashed line) and the proposed strain sensor (solid line)

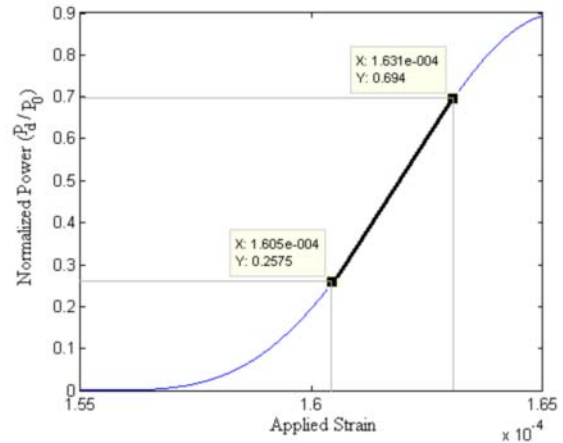


Figure 4. The linear zone of the characteristics curve of the sensor

In Figure 4 we have depicted the linear zone of the strain sensor which has the maximum slope comparing to the other zones of the characteristics curve. In this figure we take the linearity criterion of 1% to obtain the linear zone which the sensor settled to operate. From the figure we see that the sensor have to operate between the strain range of  $1.605 \times 10^{-4}$  to  $1.631 \times 10^{-4}$ . In this zone the slope of the curve is  $0.916 \times 10^3$  (normalized power/strain). Considering the laser source power of 100 mw the slope of the sensor becomes  $0.916 \times 10^2$  (W/ $\epsilon$ ). Using a pin diode with resolution of  $100\mu\text{w}$  our proposed sensor's resolution will be  $0.11\mu\epsilon$ .

## 5. Conclusion

In this paper, a novel fiber-optic strain sensor has been demonstrated. This sensor was based on the Mach-Zehnder interferometer and the concept of the displacement sensor. The combination of several effects in altering the detected power by varying the applied strain, make the proposed sensor more sensitive compared to the previous setups. It was shown that the characteristics curve of the sensor has some linear zones and the zone with the maximum slope is selected.

**Acknowledge:** The authors acknowledge the research deputy office of Sharif University of

Technology for financial support of this project and Dr. E. Lotfi for his useful comments.

## 6. References

- [1] Y.J. Rao, D.A. Jackson, "Recent progress in fiber optic low-coherence Interferometry", *Meas. Sci. Technol.* 7 (1996) pp. 981.
- [2] L.B. Yuan, L.M. Zhou, W. Jin, C.C. Chan, "Recent progress of white light interferometric fiber optic strain sensing techniques", *Rev. Sci. Instrum.* 71 (12) (2000) pp. 4648.
- [3] L.B. Yuan, F. Ansari, "White light interferometric fiber optic distribution strain sensing system", *Sens. Actuators A* 63 (1997) pp. 177.
- [4] L.B. Yuan, L.M. Zhou, "1×N star coupler as distributed fiber optic strainsensor using in white light interferometer", *Appl. Opt.* 37 (1998) pp. 4168.
- [5] L.B. Yuan, L.M. Zhou, W. Jin, "Quasi-distributed strain sensing with white-light interferometry: a novel approach", *Opt. Lett.* 25 (15) (2000) pp. 1074–1076.
- [6] L.B. Yuan, Q. Wen, C. Liu, Y. Jie, G. Li, "Twin multiplexing strain sensing array based on a low-coherence fiber optic Mach–Zehnder interferometer", *Sens. Actuators A* 90 (2006) pp. 177.
- [7] V.M. Murukeshan, P.Y. Chan, L.S. Ong, A. Asundi, "Effects of different parameters on the performance of a polarimetric sensor for smart structure applications", *Sens. Actuators A* 80 (1999) pp. 235–249.
- [8] A.S. Gerges, T.P. Newson, D.A. Jackson, "Coherence tuned fiber optic sensing system, with self-initialization, based on multimode laser diode", *Appl. Opt.* 29 (1990) pp. 4473–4480.
- [9] L. Yuan, "White light interferometric fiber-optic strain sensor from three peak wavelength broadband LED source", *Appl. Opt.* 36 (1997) pp. 6246–6250.
- [10] M. Noshad, H. Hedayati and A. Rostami, "A Proposal for High-Precision Fiber Optic Displacement Sensor", *Proceedings of Asia-Pacific Microwave Conference*, Dec 2006.
- [11] A. Rostami, M. Noshad, H. Hedayati, A. Ghanbari and F. Janabi-Sharifi, "A Novel and High-Precision Optical Displacement Sensor", *International Journal of Computer Science and Network Security*, vol.7 no.4, pp. 311-318, Apr. 2007
- [12] C.D. Butter, G.B. Hocker, "Fiber optics strain gauge", *Appl. Opt.* 17, (1978) pp. 2867–2869.
- [13] D.A. Pinnow, *Elastooptical materials*, in: R.J. Pressley *Handbook of Lasers*, CRC Press, Cleveland, OH, 1971.